LILRB4-targeting Antibody–Drug Conjugates for the Treatment of Acute Myeloid Leukemia

Yasuaki Anami[1], Mi Deng[2], Xun Gui[1], Aiko Yamaguchi[1], Chisato M. Yamazaki[1], Ningyan Zhang[1], Cheng Cheng Zhang[2], Zhiqiang An[1], and Kyoji Tsuchikama[1]

ABSTRACT

Acute myeloid leukemia (AML) is the most common and aggressive blood cancer in adults. In particular, significant unmet medical needs exist for effective treatment strategies for acute myelomonocytic leukemia (M4) and acute monocytic leukemia (M5) AML subtypes. Antibody–drug conjugates (ADC) are a promising drug class for AML therapy, as demonstrated by the FDA-approved anti-CD33 ADC, gemtuzumab ozogamicin (Mylotarg). However, CD33 is expressed in normal hematopoietic stem cells, highlighting the critical need to identify AML-specific targets to minimize the risk of potential adverse effects. We have demonstrated that the leukocyte immunoglobulin-like receptor subfamily B4 (LILRB4) is expressed at significantly higher levels on monocytic M4 and M5 AML cells than on normal counterparts. Here, we test whether LILRB4 is a promising ADC target to kill monocytic AML cells while sparing healthy counterparts. To this end, we generated ADCs from a humanized anti-LILRB4 mAb and the antimitotic payload, monomethyl auristatin F. The conjugates constructed were characterized and evaluated for LILRB4-specific cell killing potency, toxicity to progenitor cells, pharmacokinetics, and therapeutic efficacy. Our ADC linker technology platform efficiently generated homogeneous anti-LILRB4 ADCs with defined drug-to-antibody ratios. The homogeneous anti-LILRB4 ADCs demonstrated the capacity for LILRB4-mediated internalization, suitable physicochemical properties, and high cell killing potency against LILRB4-positive AML cells. Importantly, our data indicate that these ADCs spare normal progenitor cells. One of our homogeneous conjugates exerted a remarkable therapeutic effect and no significant toxicity in a xenograft mouse model of disseminated human AML. Our findings highlight the clinical potential of anti-LILRB4 ADCs in monocytic AML therapy.

Introduction

Acute myeloid leukemia (AML) is the most common acute leukemia in adults and a common pediatric cancer. Despite treatment, most patients relapse and succumb to disease within 5 years. Monocytic AML, including acute myelomonocytic leukemia (M4) and acute monocytic leukemia (M5), accounts for approximately 30% of all cases of AML (1). Patients with AML with a significant monocytic component are more likely to have evidence of extramedullary disease (1) and hyperleukocytosis (2), which is associated with a poor prognosis. In addition, clinical studies suggest that monocytic AML carries a greater risk for marrow and extramedullary relapse after stem cell transplant compared with nonmonocytic subtypes (3).

The FDA has recently approved several new drugs for AML, targeting CD33, isocitrate dehydrogenase 1 (IDH1), IDH2, FMS-like tyrosine kinase 3 (Flt3), BCL-2, and Hedgehog (4). The BCL-2 inhibitor, venetoclax, along with azacytidine is an emerging standard of care for patients more than 65 years of age and patients with comorbid conditions precluding intensive chemotherapy (5). However, a recent report demonstrates that the M5b subtype (acute monoblastic leukemia) is associated with resistance to venetoclax (6). The IC_{50} value for venetoclax is significantly higher in M5b subtype than in other AML subtypes. Thus, there is a significant unmet medical need for effective treatment strategies for monocytic AML, particularly M4 and M5 subtypes that are associated with high risks for relapse after stem cell transplant and resistance to current therapies.

Antibody–drug conjugates (ADC) are emerging chemotherapeutic agents for treating cancers including AML (7). ADCs consist of mAbs conjugated with cytotoxic agents (payloads) through stable chemical linkers. Properly designed ADCs can selectively deliver payloads to target tumor cells, resulting in improved potency, broad therapeutic window, and prolonged circulation life compared with conventional drug classes for chemotherapy. Eight ADCs have been approved by the FDA and more than 100 ADCs are currently in clinical trials. Gemtuzumab ozogamicin (Mylotarg) is the first ADC approved for the treatment of newly diagnosed or refractory CD33-positive AML (8). While promising, Mylotarg was originally withdrawn from the market in 2010 because of unexpected safety issues. It was reapproved in 2017 for patients with relapsed or refractory CD-33 positive AML with a lower dose and a modified schedule (9). CD33 is expressed not only in AML blasts, but also in normal hematopoietic stem cells (HSC; ref. 10). This lack of specificity likely contributes to the narrow therapeutic window of any anti-CD33 agents. Several other AML receptors, including CD123 (11) and C-type lectin-like molecule-1 (CLL-1; ref. 12), are being tested as ADC targets. However, CD33 is the sole target that has been clinically validated so far for AML therapy using ADCs.

[1]Texas Therapeutics Institute, The Brown Foundation Institute of Molecular Medicine, The University of Texas Health Science Center at Houston, Houston, Texas. [2]Department of Physiology, The University of Texas Southwestern Medical Center, Dallas, Texas.

Note: Supplementary data for this article are available at Molecular Cancer Therapeutics Online (http://mct.aacrjournals.org/).

Y. Anami, M. Deng, and X. Gui contributed equally to this article.

Corresponding Authors: Kyoji Tsuchikama, The University of Texas Health Science Center at Houston, 1881 East Road, Houston, TX 77054. Phone: 713-486-5431; E-mail: Kyoji.Tsuchikama@uth.tmc.edu; Cheng Cheng Zhang, Department of Physiology, The University of Texas Southwestern Medical Center, 6001 Forest Park Road, Dallas, TX 75390. E-mail: Alec.Zhang@UTSouthwestern.edu; and Zhiqiang An, E-mail: Zhiqiang.An@uth.tmc.edu

Mol Cancer Ther 2020;19:2330–9

doi: 10.1158/1535-7163.MCT-20-0407

Another concern with Mylotarg is its heterogeneous molecular composition. Mylotarg is prepared by stochastic lysine coupling, yielding a heterogeneous mixture of conjugates that differ in conjugation site and drug-to-antibody ratio (DAR). Heterogeneous antibody–drug conjugation can lead to poor pharmacokinetics, efficacy, and safety profiles (13). Collectively, ADCs targeting AML-specific antigens highly likely lead to more effective AML therapy with broader therapeutic indices than does Mylotarg. Ideally, such ADCs should be prepared by site-specific antibody–drug conjugation to overcome the issues associated with ADC heterogeneity. So far, a few ADCs, including SGN-CD123A (14) and IMGN632 (11), have been developed on the basis of these molecular design strategies.

The leukocyte immunoglobulin-like receptor subfamily B (LILRB) is a group of type I transmembrane glycoproteins expressed by normal and malignant human cells of the myelomonocytic origin (15). Because of the negative roles of phosphatases in immune activation, LILRBs are considered to be immune checkpoint factors (16). The most restrictively expressed member of the LILRB family is LILRB4. LILRB4 is expressed on normal monocytic cells (monocytes, macrophages, and some dendritic cells; ref. 15) and to a lesser extent on plasmablasts (17). LILRB4 is not expressed on neutrophils, other myeloid cells, or hematopoietic stem or progenitor cells (18). LILRB4 is expressed at significantly higher levels on monocytic AML cells than on normal counterparts, and its level inversely correlates with overall survival of patients with AML (18–20). Importantly, we have discovered that LILRB4 supports tumor development by facilitating leukemia cell infiltration into tissues and by suppressing T-cell activity through the ApoE/LILRB4/SHP2/NFκB/uPAR/ARG1 axis in AML cells (19). Furthermore, we have studied anti-LILRB4–blocking antibodies and chimeric antigen receptor-T cells that can efficiently inhibit AML development in various mouse models including humanized and patient-derived xenografted mice (18, 19). LILRB4 thus, represents an attractive target for treating monocytic AML to achieve effective and safe targeted therapy.

Here, we show that the branched linker (21–24) and glutamic acid–valine–citrulline (EVCit) linker technologies (25) developed by our group efficiently provide anti-LILRB4 ADCs with high homogeneity, desirable physicochemical properties, high cell killing potency against AML cells, and marginal toxicity to normal progenitor cells. We also demonstrate that our conjugates exert a significant therapeutic effect in a mouse model of disseminated human AML. Our findings highlight the clinical potential of our anti-LILRB4 ADCs in AML therapy.

Materials and Methods

Preparation of human mAbs with an N297A or N297Q mutation

We expressed the humanized anti-LILRB4 mAb, h128-3 (IgG1, wild-type), as described previously (26). Site-directed mutagenesis was performed to make N297A and N297Q Fc variants. The N297A variant mAb contains an alanine (A) at the amino acid residue 297 (European numbering system) in the CH2 region of the wild-type h128-3 heavy chain. The N297Q variant mAb contains a glutamine (Q) at this position. The constructs for the mutated heavy chain and wild-type light chain were cotransfected into human embryonic kidney freestyle 293 cells (HEK293F, Thermo Fisher Scientific) using Polyethyleneimine (Sigma) as a transfection reagent. Seven days after cotransfection, supernatants were harvested and antibodies were purified by affinity chromatography using Protein A Resin (Repligen) as reported previously.

Cell lines

Human monocytic AML cell lines, THP-1 (TIB-202), MV4-11 (CRL-9591), and U937 (CRL-1593.2), were purchased from the ATCC within the period of 2010 to 2018, characterized by the manufacturer using routine DNA profiling, and no further authentication was conducted by the authors. All cell lines were routinely tested using a Mycoplasma Contamination Kit (R&D Systems) to make sure there was no contamination in cell cultures and passaged before becoming fully confluent up to 20 passages.

LILRB4 internalization assay

THP-1 or MV4-11 cells were seeded in 24-well plates (5×10^4 cells/well, 1 mL) and incubated with N297A and N297Q Fc variants (5 μg/mL) at 37°C for 24 hours. Subsequently, cells were blocked with 300 μg/mL human IgG (generated in-house) at 4°C for 1 hour. Finally, surface LILRB4 was stained with a noncompetitive rabbit anti-LILRB4 antibody R193 (5 μg/mL, generated in-house), incubated with 1:200 diluted 488-conjugated goat $F(ab')_2$ anti-rabbit $F(ab')_2$ (Jackson ImmunoResearch Laboratories), and quantified by FACS. The degree of internalization was calculated by dividing the signal from the sample treated with anti-LILRB4 antibodies by the signal from the sample treated with PBS. This value was expressed as a percentage.

Microbial transglutaminase–mediated antibody–linker conjugation

Anti-LILRB4 IgG1 with a N297A or N297Q mutation or an in-house–generated isotype control (330 μL in PBS, 17.2 mg/mL, 5.68 mg antibody) was incubated with a diazidoamine branched linker (refs. 21, 22; 30.3 μL of 100 mmol/L stock solution in water, 80 equivalent) and Activa TI (90 μL of 40% w/v solution in PBS, Ajinomoto, purchased from Modernist Pantry) at room temperature overnight. The reaction was monitored by LC/MS equipped with a MabPac RP Column (3 × 50 mm, 4 μm, Thermo Fisher Scientific). Elution conditions were as follows: mobile phase A, water (0.1% formic acid); mobile phase B, acetonitrile (0.1% formic acid); gradient over 6.8 minutes from A:B, 75:25 to 1:99; and flow rate, 0.4 mL/minute. The conjugated antibodies were purified by size-exclusion chromatography (SEC, Superdex 200 increase 10/300 GL, GE Healthcare; solvent, PBS and flow rate, 0.6 mL/minute) to afford pure, monomeric, and homogeneous antibody–linker conjugates [5.50 mg, >95% yield determined by bicinchoninic acid (BCA) assay].

Strain-promoted azide−alkyne cycloaddition for payload installation

DBCO–peg_3–EVCit–PABC–MMAF (44 μL of 4 mmol/L stock solution in DMSO, 1.5 equivalent per azide, synthesized according to our previous article; ref. 25) was added to a solution of each mAb–linker conjugate in PBS (840 μL, 5.2 mg/mL). The mixture was incubated at room temperature for 2 hours. The reaction was monitored by LC/MS equipped with a MabPac RP column and the crude products were purified by SEC. Anti-LILBR4 and nontargeting ADCs with a DAR of 4 were obtained from the corresponding N297A–linker conjugates; anti-LILRB4 ADCs with a DAR of 8 were obtained from the N297Q mAb–linker conjugate (>95% yield in both cases, determined by BCA assay). Analysis and purification conditions were the same as described above. Average DAR values were determined by reverse-phase high-performance liquid chromatography (HPLC, based on UV peak areas at 280 nm). Nontargeting ADCs were prepared in the same manner. Purified ADCs were formulated in PBS or citrate buffer (20 mmol/L sodium citrate and 1 mmol/L citric

acid, pH 6.6) containing 0.1% Tween 80 and trehalose (70 mg/mL) and stored at 4°C until use (for up to a month).

Long-term stability test

Each ADC (1 mg/mL, 100 μL) in PBS was incubated at 37°C. An aliquot (10 μL) was taken after 28 days and analyzed using an Agilent 1100 HPLC System equipped with a MAbPac SEC-1 Analytic Column (4.0 × 300 mm, 5 μm, Thermo Fisher Scientific). The conditions were as follows: solvent, PBS and flow rate, 0.2 mL/minute.

Hydrophobic interaction chromatography analysis

Each ADC (1 mg/mL, 10 μL in PBS) was analyzed using an Agilent 1100 HPLC System equipped with a MAbPac HIC-Butyl Column (4.6 × 100 mm, 5 μm, Thermo Fisher Scientific). Elution conditions were as follows: mobile phase A, 50 mmol/L sodium phosphate containing ammonium sulfate (1.5 mol/L) and 5% isopropanol (pH 7.4); mobile phase B, 50 mmol/L sodium phosphate containing 20% isopropanol (pH 7.4); gradient over 30 minutes from A:B, 99:1 to 1:99; and flow rate, 0.5 mL/minute.

ELISA binding assay

Corning 96-well EIA/RIA plates were coated overnight at 4°C with human LILRB4 recombinant protein (rhLILRB4-his, 1 μg/mL, Sino Biologicals) and blocked for 2 hours at 37°C with 5% nonfat milk. Serial dilutions of anti-LILRB4 antibodies (h128-3-N297A mAb, DAR-4 ADC, DAR-8 ADC, and hIgG isotype control, 100 μL each) were added and incubated for 2 hours at room temperature. Subsequently, the plates were washed with PBS-Tween 20 (0.05%) three times and then incubated for 1 hour with horseradish peroxidase–conjugated anti-hFc Antibody (Jackson ImmunoResearch Laboratories) at room temperature. Finally, TMB substrate (Sigma) was added to each well. Color development was stopped with 2 mol/L sulfuric acid and absorbance in each well (at 450 nm) was recorded using a Plate Reader (Molecular Devices).

Cell viability assay

THP-1, MV4-11, and U937 cells were cultured in RPMI1640 supplemented with 10% FBS at 37°C under 5% CO_2 and atmospheric O_2 levels. To test the effects of ADCs on cell growth, 5,000 cells were cultured in each well of 96-well plate and treated with indicated drugs or ADCs for 5 days. Propidium iodide (10 μg/mL) was added to the treated cells, and then live cells (propidium iodide negative) were counted using a Flow Cytometer (FACSCalibur, BD Biosciences). EC_{50} values were determined by nonlinear curve fitting (4-variable parameters) using GraphPad Prism 8 software.

Colony-forming unit assay

Human umbilical cord blood $CD34^+$ cells (Stemcell Technologies, catalog no., 70008.5) or THP-1 cells (400 cells each) were treated with serial diluted concentrations of an indicated mAb or ADC, resuspended in MethoCult Classic (Stemcell Technologies, catalog no., 4434), plated, and incubated in a humidified chamber as per the manufacturer's directions. Colonies were classified and counted after 8 days.

In vivo pharmacokinetics study

Animal work described in this article was approved and conducted under the oversight of the University of Texas Southwestern (Dallas, TX, UTSW) Institutional Animal Care and Use Committee. In each study, age-matched (4–8 weeks) female mice were used and randomly allocated to each group. The minimum number of mice in each group was calculated on the basis of the results from our prior relevant studies (19). NOD-scid IL2Rγ null (NSG) mice were purchased from and maintained at the Animal Core Facility of UTSW (Dallas, TX). NSG mice were injected intravenously with 1×10^6 human leukemia cells on day 0 and 30 mg/kg of normal human IgG (Innovative Research) for preconditioning on day 6. Low doses of antibody-based therapeutics in mice lacking endogenous antibodies have reportedly suffered from a severely impaired half-life in circulation (27). Preconditioning using IgG has been established as a means to overcome this issue in NSG mice. On day 7, animals were injected with a single dose of unconjugated mAb or ADCs (3 mg/kg) via the tail vein. Blood samples were collected into tubes at 15 minutes, 6 hours, 24 hours, 48 hours, 96 hours, 216 hours, and 336 hours after injection (5 animals/timepoint). After being centrifuged at 1,500 × *g* for 10 minutes, plasma fractions were transferred to sterile cryovials, aliquoted, and stored at −80°C until analysis. Plasma concentrations of anti-LILRB4 mAb and monomethyl auristatin F (MMAF) ADCs were determined by ELISA. Antibody and ADCs in the diluted plasma samples were captured on ELISA plates precoated with LILRB4 recombinant protein (2 μg/mL) for total anti-LILRB4 antibody detection or with anti-MMAF polyclonal antibodies (1 μg/mL, Levena Biopharma) for intact ADC detection. Alkaline phosphatase–conjugated goat anti-human IgG $F(ab)_2$ (Jackson ImmunoResearch Laboratories) was used as a detection antibody with 1:5,000 dilution. Fluorescence signals were developed with a substrate solution of 4-MUP (Sigma) and recorded using a microplate reader (excitation, 340 nm and emission, 460 nm). AUC was calculated using GraphPad Prism 8 software.

In vivo treatment study

Xenografted mice were prepared essentially as described above. Briefly, 6- to 8-week-old NSG mice were used for transplantation. THP-1 cells stably expressing luciferase (ref. 19; 1×10^6 cells) were resuspended in 200 μL PBS for each mouse. All mice were preconditioned with 30 mg/kg human IgG (i.v.) 24 hours before ADC injection. Subsequently, mice were given the ADC drugs indicated or control IgG intravenously at days 7, 14, and 21 after transplantation. Leukemia growth was monitored by bioluminescence imaging using an IVIS *in vivo* imager (Max, 3×10^8 p/second/cm^2/sr and Min, 5×10^6 p/second/cm^2/sr). Bioluminescence imaging and body weight measurement were performed every 3 or 4 days. All animals were monitored daily and deaths were recorded when moribund animals were euthanized or found dead. Kaplan–Meier survival curve statistics were analyzed using the log-rank (Mantel–Cox) test.

Results

Construction and characterization of anti-LILRB4 ADCs

Receptor-mediated internalization is a key mechanism by which ADCs exert a cytotoxic effect upon intracellular release of payloads. We sought to test whether the anti-LILRB4 mAb, h128-3, with a N297A- or N297Q-Fc mutation could internalize upon binding to LILRB4 on leukemia cells. Toward this end, we quantified LILRB4 expressed on the surface of THP-1 and MV4-11 cells before and after being treated with these antibodies or an isotype control for 24 hours (**Fig. 1**). The surface LILRB4 levels were consistent at 4°C in either case (Supplementary Fig. S1). However, the surface LILRB4 levels decreased after incubation with either N297A or N297Q mAb at 37°C for 24 hours, indicating that these mAbs were internalized. The observed time- and temperature-dependent internalization indicates that binding of these mAbs to LILRB4 triggers receptor-mediated

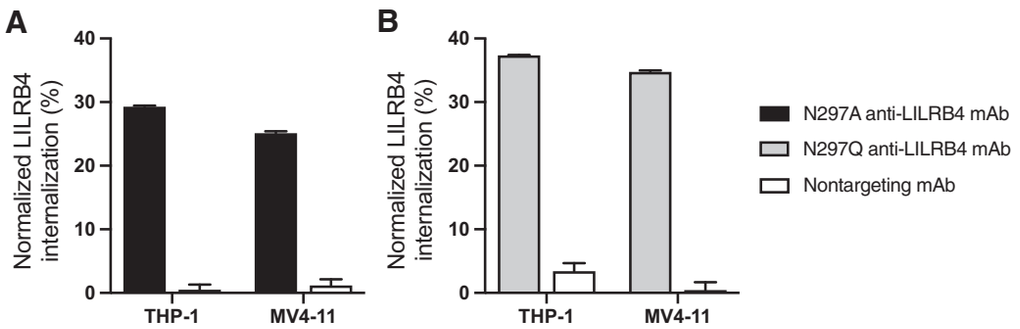

Figure 1.
Internalization of anti-LILRB4 mAb–surface LILRB4 complex. THP-1 and MV4-11 cells were treated with anti-LILRB4 Fc variants with N297A (black; **A**) or N297Q mutation (gray; **B**) at 37°C for 24 hours before surface LILRB4 was quantified by FACS. A nontargeting mAb (white) was also tested in each assay. The degree of internalization is normalized to the expression level of surface LILRB4 treated with PBS. All assays were performed in duplicate. Error bars represent mean ± SEM.

endocytosis (28). The nontargeting control was not efficiently internalized into either cell type even at elevated temperature.

On the basis of the findings above, we set out to generate LILRB4-targeting ADCs from these mAbs using the homogeneous antibody–drug conjugation technologies developed by our group (**Fig. 2A**; refs. 21, 22). First, we introduced branched diazidoamine linkers onto the Fc variants of h128-3 mAb at glutamine 295 (Q295) by microbial transglutaminase (MTGase)-mediated conjugation. The branched linker was also introduced at Q297 in the case of the mAb with a N297Q mutation. This high-yielding conjugation provided homogeneous mAb–branched linker conjugates from both Fc variants. Subsequently, we installed the antimitotic agent MMAF onto the linker conjugates by strain-promoted azide–alkyne click reaction. To this end, we used a payload module consisting of dibenzocyclooctyne (DBCO), polyethylene glycol (PEG) spacer, glutamic acid–valine–citrulline (Glu–Val–Cit) cleavable linker, *p*-aminobenzyloxycarbonyl (PABC) group, and MMAF (Supplementary Fig. S2A). MMAF is usually conjugated with maleimide-based non-cleavable linkers based on the general assumption that cleavable valine–citrulline (Val–Cit)–MMAF can undergo premature payload

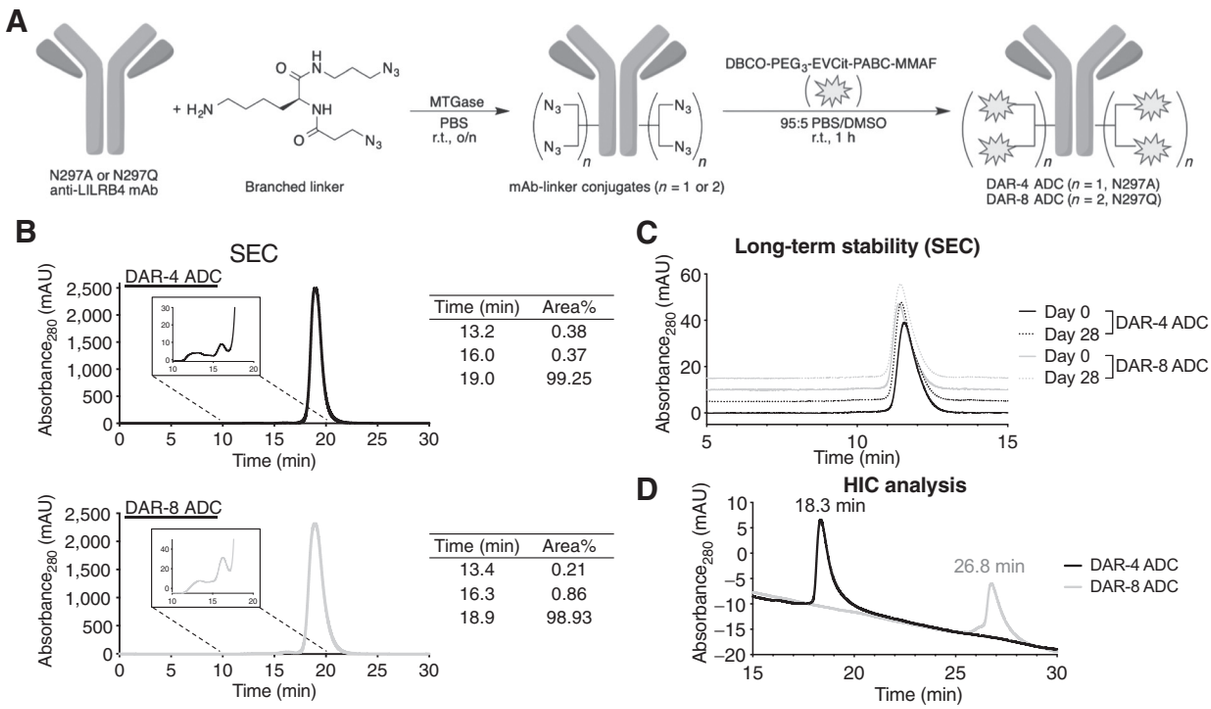

Figure 2.
Construction and characterization of homogeneous anti-LILRB4 ADCs. **A,** Construction of DAR-4 and DAR-8 ADCs by MTGase-mediated branched linker conjugation and following strain-promoted azide–alkyne cycloaddition (spark: DBCO–PEG_3–EVCit–PABC–MMAF module). **B,** Preparative SEC traces of DAR-4 and DAR-8 ADCs. **C,** Analytical SEC traces of DAR-4 and DAR-8 ADCs after incubation in PBS at 37°C for 28 days. **D,** HIC analysis under physiologic conditions (phosphate buffer, pH 7.4).

release in circulation prior to reaching target tumors. However, we have uncovered that our branched linker system requires the cleavable Glu–Val–Cit sequence to maximize ADC efficacy *in vivo* (25). Encouragingly, this linker can prevent premature linker degradation in human and mouse plasma. In addition, our conjugation method does not rely on cysteine–maleimide coupling, which is known to undergo deconjugation and loss of payload in circulation (29). These features assure the validity of our ADC design. We obtained homogeneous DAR-4 and DAR-8 ADCs from the mAbs in a quantitative manner. Average DARs of these ADCs were determined to be 4 and 8, respectively (Supplementary Fig. S2B and S2C). We also prepared nontargeting ADC as an isotype control constructed using the same payload module (DAR: 4) in the same manner. SEC analysis showed that both anti-LILRB4 ADCs existed predominantly in the monomer form (**Fig. 2B**). In addition, no significant aggregation was observed for both ADCs after incubation at 37°C in PBS for 28 days, demonstrating their long-term thermal stability (**Fig. 2C**). Hydrophobicity of the ADCs was also assessed by hydrophobic interaction chromatography (HIC) analysis (**Fig. 2D**). We confirmed that the DAR-8 ADC (26.8 minutes) was much more hydrophobic than the DAR-4 ADC (retention time, 18.3 minutes) because of the increased number of hydrophobic MMAF.

In vitro evaluation of the ADCs for LILRB4-dependent binding and cytotoxicity

We determined the binding affinity of the anti-LILRB4 ADCs constructed for recombinant human LILRB4 by ELISA (Supplementary Fig. S3). Both DAR-4 and -8 ADCs showed similar binding affinity (K_D, 0.16 and 0.21 nmol/L, respectively) to the parental N297A Fc variant (K_D, 0.15 nmol/L). This result indicates that conjugating the branched linker and MMAF components at Q295 (and Q297 in the case of the N297Q mAb) within the Fc region did not impact the

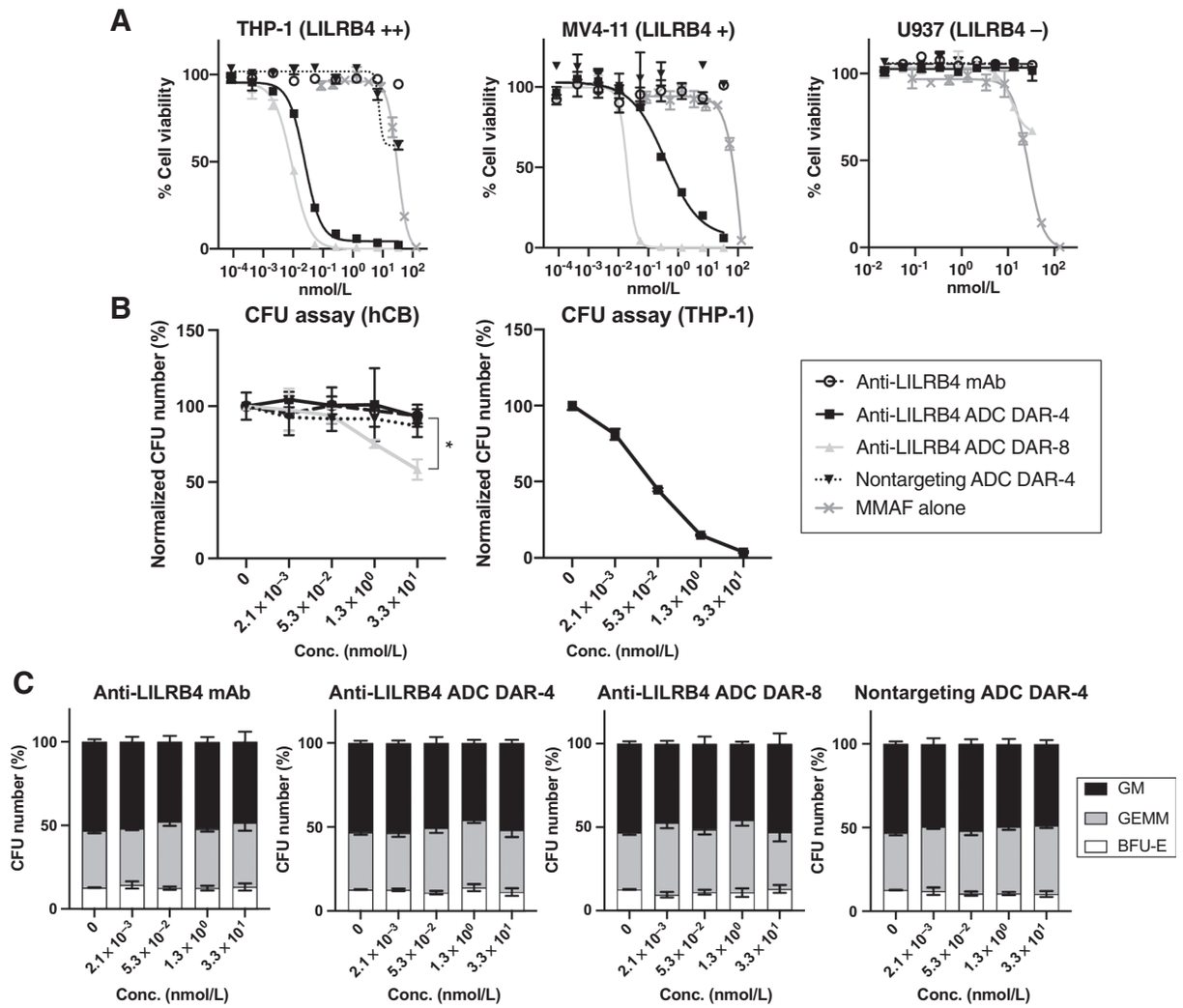

Figure 3.

In vitro cytotoxicity of anti-LILRB4 mAb h128-3, DAR-4 ADC, DAR-8 ADC, and nontargeting DAR-4 ADC (isotype control). **A,** Cell killing potency in the AML cell lines THP-1, MV4-11, and U937. **B,** CFU assay in THP-1 or UCB-CD34 cells. **C,** CFU numbers of BFU-E (white), CFU-GEMM (GEMM, light gray), and CFU-GM (GM, dark gray) after being treated with each mAb or ADC. CFU numbers are normalized to the count of a untreated group. All assays were performed in triplicate. Error bars represent mean ± SEM. *, $P < 0.05$ (DAR-4 vs. DAR-8 in hCB, Welch *t* test). hCB, human cord blood.

LILRB4 antigen binding. This result is consistent with our previous report using anti-HER2 mAbs (25).

We then performed an *in vitro* cytotoxicity assay using three AML cell lines with varying LILRB4 expression levels: THP-1 (AML, LILRB4^{++}), MV4-11 (LILRB4^{+}), and U937 (LILRB4^{-}; **Fig. 3A**; Supplementary Table S1). Live and dead cells were counted by flow cytometry after a 5-day treatment with each conjugate. As anticipated, MMAF alone did not show high potency or target specificity in either cell line. Importantly, both DAR-4 and -8 ADCs could efficiently kill THP-1 and MV4-11 cells. In particular, the DAR-8 ADC exerted much greater potency (EC_{50}, 9.3 pmol/L in THP-1 and 19.7 pmol/L in MV4-11) than the DAR-4 variant (EC_{50}, 25 pmol/L in THP-1 and 374 pmol/L in MV4-11). As expected, the unmodified anti-LILRB4 mAb and a nontargeting ADC prepared from an isotype control (DAR-4) showed a marginal cell killing effect in these LILRB4-positive cells. U937 cells have no detectable LILRB4 expression, and correspondingly, no cytotoxicity was observed following incubation with the DAR-4 ADC, the nontargeting ADC, or the unmodified mAb. The DAR-8 ADC showed moderate cytotoxicity only at very high concentrations (>10 nmol/L). This result suggests that a limited amount of DAR-8 is internalized. We next evaluated the ADCs for potential on-target off-tumor toxicity against CD34^{+} umbilical cord blood cells (UCB-CD34) in a colony-forming unit (CFU) assay (**Fig. 3B**). There were no differences in the colony number when cells were treated with increased concentrations of the unmodified anti-LILRB4 mAb, DAR-4 ADC, or nontargeting ADC, whereas the DAR-8 ADC showed moderate toxicity only at very high concentrations (>5,000 ng/mL or >30 nmol/L). None of the treatments had major effects on the contributions of BFU-erythroid (E), CFU-granulocyte monocyte (GM), or CFU-granulocyte-erythroid-monocyte-megakaryocyte (GEMM) colony numbers (**Fig. 3C**). These results demonstrate that our anti-LILRB4 ADCs, in particular the DAR-4 ADC, can selectively kill LILRB4-positive monocytic AML cells while sparing off-target progenitor cells.

In vivo evaluation of the ADCs for pharmacokinetics and therapeutic efficacy

We further evaluated the anti-LILRB4 ADCs in a mouse model of human AML. Seven days after NSG mice received THP-1 cells intravenously, each conjugate was administered at 3 mg/kg via the tail vein. For pharmacokinetics evaluation, blood samples were collected periodically. After extracting serum, we performed sandwich ELISA to determine the serum concentration of total antibody (**Fig. 4A**; Supplementary Table S2). The unmodified mAb and the DAR-4 ADC showed comparable clearance rates and AUC. In contrast, the DAR-8 ADC was cleared at a faster rate, resulting in significantly reduced AUC. This rapid clearance is likely caused by the increased hydrophobicity as seen in the HIC analysis. These results show that the DAR-8 ADC possesses an undesirable pharmacokinetics profile.

Finally, we tested the LILRB4-targeting ADCs for *in vivo* treatment efficacy in a mouse model of human AML. THP-1 cells that stably expressed luciferase were intravenously injected into NSG mice to establish a disseminated AML model. At 7 days after transplantation, each conjugate (3 mg/kg) was administered weekly for the first 3 weeks (**Fig. 4B** and **C**). Both DAR-4 and -8 ADCs exerted therapeutic effect with statistically significant survival benefits (Supplementary Table S3). Notably, the DAR-8 ADC was inferior to the DAR-4 ADC. The poor pharmacokinetics profile of the DAR-8 ADC may account for the reduced efficacy despite increased DAR. There were no obvious differences in body weight between the mAb and ADC treatment groups (Supplementary Fig. S4), suggesting that the ADC treatment did not cause significant acute toxicity in this model.

Discussion

Although the anti-CD33 ADC, gemtuzumab ozogamicin (Mylotarg), was reapproved in 2017 (9), efforts to establish anti-CD33 therapies for AML have been frustrated by the narrow therapeutic indices due to broad expression of CD33 in normal HSCs (30). Indeed, clinical trials for vadastuximab talirine (SGN-CD33A), another anti-CD33 ADC, have recently been discontinued because of increased fatality rates (31). Thus, exploration of novel targets is critically needed to establish ADC-based AML therapies with improved efficacy and safety. CLL-1, a novel AML target, was recently tested in ADC-based efficacy studies (12). An anti-CD123 ADC (IMGN632) is currently in clinical trials for AML treatment (11). However, CD123 is also expressed on normal HSCs, raising safety concerns similar to those for anti-CD33 therapies (30). Indeed, a phase I study for the anti-CD123 ADC, SGN-CD123A, was unsuccessful and has been terminated because of safety concerns in patients with AML (NCT02848248).

We have been studying the function and signaling of LILRBs in cancer development. We and others have demonstrated that several immunoreceptor tyrosine-based inhibition motif receptors including LILRB1, LILRB2, LILRB4, and LAIR1 support development of leukemia and other cancers (15, 18, 19, 32–36). Several LILRBs were ranked as AML target candidates (37). Results of our previous studies suggested that LILRBs have dual roles as immune checkpoint molecules and as tumor-sustaining factors (15). In particular, LILRB4 is expressed on monocytic lineages with significantly higher levels of expression on leukemia cells than on normal monocytes, HSCs, or progenitor cells (18, 19). In addition to monocytic AML, LILRB4 is known to be expressed in other hematologic malignancies, including 50% of cases of chronic lymphocytic leukemia (38) and some cases of multiple myeloma and MLL-rearranged Pre-B ALL (18, 39). Moreover, LILRB4 was reported to be expressed on myeloid-derived suppressor cells (40), tolerogenic dendritic cells (41), and tumor-associated macrophages (15, 32), which are components of the immunosuppressive tumor microenvironment (42–44). Certain solid organ tumors, such as colorectal carcinoma, pancreatic carcinoma, and melanoma, have soluble LILRB4 detected that may inhibit T-cell immunity *in vitro* (15). Collectively, these considerations show that LILRB4 represents an ideal target for leukemia therapy with potentially minimal myelotoxicity (18–20).

We have previously identified h-128-3, a humanized anti-LILRB4 mAb generated by our group, as a potential therapeutic candidate for LILRB4-targeted immunotherapy of AML (19, 26). In addition, our initial evaluation in this report revealed that N297A and N297Q h-128-3 mAbs were efficiently internalized into LILRB4-positive AML cells via endocytosis, an initial step toward ADC target–specific cytotoxicity. Further evaluation will be needed to better understand the kinetics of this LILRB4-mediated endocytosis and the alternation of the expression level after continual treatment with anti-LILRB4 mAbs. Nonetheless, these findings encouraged us to pursue the use of the h-128-3 mAbs in the ADC format for selective delivery of potent chemotherapeutic agents to monocytic AML cells.

We prepared the anti-LILRB4 ADCs from the h-128-3 mAbs with an N297A or N297Q mutation. This mutation allows us to omit the removal of the *N*-glycan chain at N297, a necessary step for our MTGase-mediated antibody–linker conjugation at Q295 (45). More importantly, the lack of the *N*-glycan is likely advantageous in terms

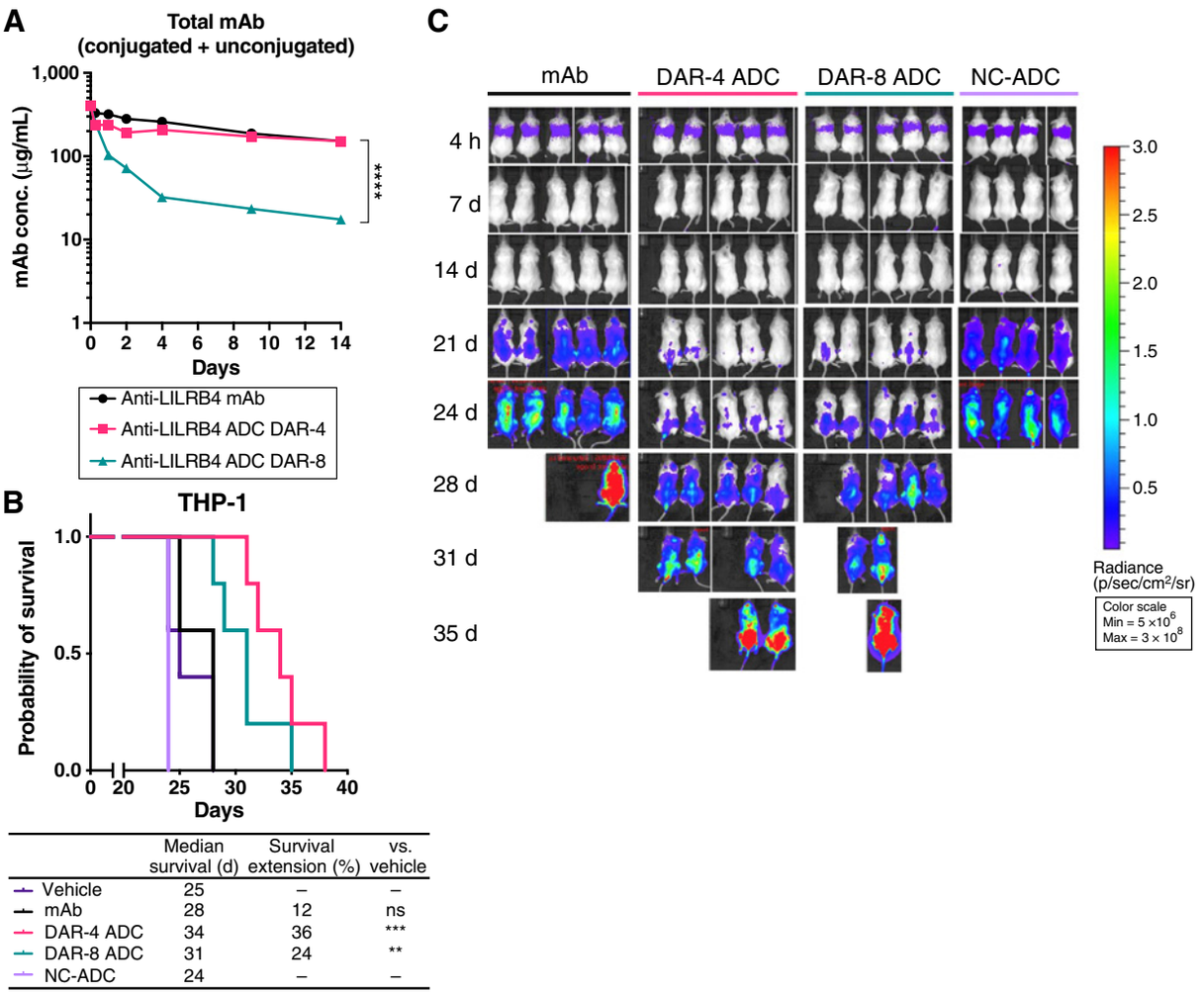

	Median survival (d)	Survival extension (%)	vs. vehicle
Vehicle	25	–	–
mAb	28	12	ns
DAR-4 ADC	34	36	***
DAR-8 ADC	31	24	**
NC-ADC	24	–	–

Figure 4.

In vivo evaluation of anti-LILRB4 ADCs. **A,** Pharmacokinetics of unmodified anti-LILRB4 mAb (black), DAR-4 ADC (magenta), and DAR-8 ADC (green) in female NSG mice ($n = 5$). Mice were injected with each drug at 3 mg/kg. At the indicated timepoints, blood was collected to quantify total antibody (conjugated and unconjugated) by sandwich ELISA. Kaplan–Meier curve (**B**) and bioluminescence images (**C**) of the THP-1 xenograft mouse model (female NSG mice), $n = 4$ for nontargeting control ADC (NC-ADC); $n = 5$ for the other groups. Mice were injected intravenously with THP-1 (1×10^6 cells) on day (d) 0 and treated with each drug (3 mg/kg) or vehicle control (purple) on days 7, 14, and 21. **, $P < 0.01$; ***, $P < 0.005$; ****, $P < 0.0001$ (DAR 4 vs. DAR 8 in pharmacokinetics analysis, Welch *t* test; survival curve, log-rank test).

of ADC toxicity profile. Studies have shown that liver toxicity associated with ADCs is caused by interactions of the antibody glycans with mannose receptors and Fcγ receptor–positive cells, leading to off-target cellular uptake (46). Given the subnanomolar potency of our ADCs in LILRB4-positive cells, and the loss of complement-dependent cytotoxicity, antibody-dependent cellular cytotoxicity (ADCC), and antibody-dependent cellular phagocytosis (ADCP) caused by omission of the *N*-glycan should minimally attenuate the overall *in vivo* efficacy. Together, the use of Fc-mutated anti-LILRB4 ADCs appears to be a practical means to broaden their therapeutic indices.

Using our conjugation technologies, we prepared anti-LILRB4 ADCs with high homogeneity that retained binding affinity to LILRB4. The DAR-8 ADC showed higher hydrophobicity than that of the DAR-4 variant. However, no significant aggregation was observed in either case even after long-term incubation at 37°C. Both DAR-4 and DAR-8 ADCs exhibited subnanomolar-level cell killing potency in LILRB4-positive AML cells (THP-1 and MV11-4), but not in LILRB4-negative cells (U937). As shown in this and other reports, MMAF alone was not capable of killing these cells at such low concentrations because of its poor membrane permeability (47). These results support our hypothesis that the h-128-3 mAb is a good vehicle for drug delivery. In our cell killing assays, the DAR-8 ADC was more than twice as potent as the DAR-4 ADC. The drug multiplicity effect was much more significant in MV4-11 cells expressing LILRB4 at a moderate level rather than in THP-1 with high LILRB4 expression. This result indicates that the number of ADC molecules delivered to THP-1 was close to saturation even at DAR 4 because of high LILRB4 expression.

The ADCs were also tested for potential on-target off-tumor toxicity against UCB-CD34. Our results clearly show that our anti-LILRB4 ADCs can spare off-target progenitor cells. Finally, our LILRB4 ADCs

were tested for therapeutic efficacy in a disseminated THP-1 model, a more clinically relevant model than subcutaneous xenograft models. N297A h-128-3 mAb provided a marginal therapeutic effect largely due to lack of Fc-mediated ADCC and ADCP (26). The DAR-4 and DAR-8 conjugates provided 36% and 24% extension of median survival time, respectively. Our prior analysis has shown that the expression level of LILRB4 in patient-derived primary monocytic AML cells is generally higher than that in THP-1 cells (19). Thus, this result indicates that our LILRB4 ADCs could exert a meaningful therapeutic effect in a majority of patients with AML. There was no acute toxicity associated with ADC administration in the mouse model. While encouraging, it has been reported that mice are more resistant to toxicity caused by auristatins than humans (48). Therefore, in-depth studies using advanced models (e.g., humanized mice and primates) are needed to determine the potential toxicity of our ADCs to the human body. In contrast to our observation in the cell killing assays, the DAR-4 ADC outperformed the DAR-8 variant in the *in vivo* model. Both of our conjugates were constructed using the Glu–Val–Cit linker system with exceptional stability in mouse circulation (25). Considering this point, the rapid clearance of DAR-8 ADC is likely caused by its increased hydrophobicity, in agreement with previous reports on *in vitro* and *in vivo* efficacy of hydrophobic high-DAR ADCs (13, 49). Although drug potency is not a negligible contributing factor, this result highlights the critical importance of the pharmacokinetics profile for *in vivo* efficacy. Conjugation technologies that enable the installation of highly potent payloads without exacerbating pharmacokinetics and biodistribution profiles could yield anti-LILRB4 ADCs with improved overall efficacy. One strategy that could allow us to achieve this goal is installation of payloads much more potent than MMAF, for instance tubulysin or pyrrolobenzodiazepine dimers. Testing such different payload types is also crucial to better understand payload-associated toxicity profiles (e.g., ocular toxicity caused by MMAF). Another strategy is masking hydrophobic high-DAR ADCs with hydrophilic long chains such as PEG (49) and polysarcosine (50).

We believe LILRB4-targeting ADCs should have only minimal toxicity compared with any other antibody-based agents based on the following reasons. (i) LILRB4 is only expressed on monocytic cells, but not on other cells including myeloid progenitors or stem cells (**Fig 3B** and **C**). Thus, the toxicity of anti-LILRB4 ADCs will be lower than other anti-AML agents with myeloablative activities. (ii) LILRB4 is much more highly expressed on monocytic AML cells than on normal monocytic counterparts (19). Therefore, our anti-LILRB4 ADCs likely have a poorer ability to kill normal monocytic cells than to monocytic AML cells. (iii) In human, low or high numbers of monocytes do not usually cause symptoms. A reasonable comparison of the potential monocytic cell depletion by our agent can be made for a disorder called the MonoMAC syndrome. MonoMAC is a rare autosomal dominant syndrome associated with monocytopenia, B and natural killer (NK) cell lymphopenia, and mycobacterial, fungal, and viral infections. In patients with MonoMAC, 12 distinct mutations in the *GATA2* gene have been identified, which include missense mutations affecting the zinc finger-2 domain and insertion/deletion mutations leading to frameshifts and premature termination. Because the *GATA2* mutations affect the activity of HSCs and multiple lineages (monocytes, B cells, and NK cells), it is unreasonable to raise a lack of monocytes as the sole factor contributing to microbial and viral infections caused by this disease. Conceptually, one would think B cells and NK cells play more important roles than monocytes in protecting against infections. Even in that scenario, the biomedical and clinical research community has seen the success of the anti-CD20 mAbs rituximab (Rituxan) as a heme-onc drug and ocrelizumab (Ocrevus) as a multiple sclerosis drug with manageable adverse effects. Collectively, even if normal monocytic cells are killed by an anti-LILRB4 ADC, the toxicity would be minimal.

In summary, we have demonstrated that targeting LILRB4 using ADCs is a promising strategy for eradicating monocytic AML cells. We expect that fine-tuning several factors, including the choice of payload and conjugation strategies, will provide more efficacious ADCs than the prototype presented in this study. This study warrants further evaluation of the anti-LILRB4 ADCs in immunocompetent models (e.g., humanized mice), more specifically, the assessment of the synergistic effect derived from its ability of immune checkpoint modulation. It is also important to evaluate these ADCs in more advanced animal models including primates to further validate the clinical translatability. Such efforts may lead to novel drug candidates with the potential to become effective and safe antitumor therapy based on targeting LILRB4.

Disclosure of Potential Conflicts of Interest

Y. Anami reports a patent for PCT/US2018/034363 issued, US-2020-0115326-A1 issued, and EU18804968.8-1109/3630189 issued. M. Deng reports other from Immune-Onc Therapeutics (holds equity in Immune-Onc Therapeutics and was listed as an inventor of several LILRB-related patents licensed to Immune-Onc Therapeutics) outside the submitted work. C.M. Yamazaki reports a patent for PCT/US2018/034363 issued, US-2020-0115326-A1 issued, and EU18804968.8-1109/3630189 issued. N. Zhang reports grants from Cancer Prevention and Research Institute of Texas (coinvestigator of the grants: RP150551 and RP190561) during the conduct of the study and Immune-Onc Therapeutics (co-principal investigator for a sponsored research agreement with Immune-Onc and the company licensed the LILRB4 antibody patent from her university), other from Immune-Onc Therapeutics (owns the company stocks through University of Texas out-licensing the patent to the company) outside the submitted work, as well as has a patent for PCT/US2016/020838 and PCT/US2017/044171 issued (patent on monoclonal antibodies targeting LILRB family members) and PCT/US2018/034363; US-2020-0115326-A1; EU18804968.8-1109/3630189 issued (ADC linker chemistry). C.C. Zhang reports grants from NIH and Cancer Prevention and Research Institute of Texas during the conduct of the study, other from Immune-Onc Therapeutics (sponsored research agreement and member of the scientific advisory board, had several patent applications licensed to Immune-One Therapeutics) outside the submitted work, as well as has a patent for PCT/US2016/020838 and PCT/US2017/044171 pending to Immune-Onc Therapeutics. Z. An reports grants from CPRIT (principal investigator on two CPRIT grants: RP150551 and RP190561), Immune-Onc Therapeutics (serves as a coinvestigator for a sponsored research agreement with Immune-Onc Therapeutics), and Welch Foundation (principal investigator of a Welch Foundation grant: AU-0042-20030616) during the conduct of the study, other from Immune-Onc Therapeutics (serves as a member of the scientific advisory board of Immune-Onc Therapeutics) outside the submitted work, as well as has a patent for yes issued (as a coinventor on two patents PCT/US2016/020838 and PCT/US2017/044171). K. Tsuchikama reports grants from Department of Defense during the conduct of the study, as well as has a patent for PCT/US2018/034363 issued, US-2020-0115326-A1 issued, and EU18804968.8-1109/3630189 issued. No potential conflicts of interest were disclosed by the other authors.

Authors' Contributions

Y. Anami: Formal analysis, validation, investigation, visualization, methodology, writing-original draft, writing-review and editing. **M. Deng:** Formal analysis, validation, investigation, visualization, methodology, writing-original draft, writing-review and editing. **X. Gui:** Formal analysis, validation, investigation, visualization, methodology, writing-original draft. **A. Yamaguchi:** Validation, investigation. **C.M. Yamazaki:** Validation, investigation. **N. Zhang:** Resources, supervision, methodology, project administration, writing-review and editing. **C.C. Zhang:** Conceptualization, resources, supervision, funding acquisition, methodology, writing-original draft, project administration, writing-review and editing. **Z. An:** Conceptualization, resources, supervision, funding acquisition,

methodology, project administration, writing-review and editing. **K. Tsuchikama:** Conceptualization, resources, supervision, funding acquisition, methodology, writing-original draft, project administration, writing-review and editing.

Acknowledgments

We thank Dr. Georgina T. Salazar for editing the article. This work was supported by the NCI grant (1R01CA248736 to C.C. Zhang), the Department of Defense (the Breast Cancer Research Program, W81XWH-18-1-0004 and W81XWH-19-1-0598 to K. Tsuchikama), the Cancer Prevention and Research Institute of Texas (DP150056 and RP180435 to C.C. Zhang; and RP150551 and RP190561 to Z. An), the Welch Foundation (AU-0042-20030616 to Z. An), the University of Texas System (Regents Health Research Scholars award to K. Tsuchikama), and the Japan Society for the Promotion of Science (postdoctoral fellowship to Y. Anami and A. Yamaguchi).

The costs of publication of this article were defrayed in part by the payment of page charges. This article must therefore be hereby marked *advertisement* in accordance with 18 U.S.C. Section 1734 solely to indicate this fact.

Received May 14, 2020; revised July 9, 2020; accepted August 25, 2020; published first September 2, 2020.

References

1. Ganzel C, Manola J, Douer D, Rowe JM, Fernandez HF, Paietta EM, et al. Extramedullary disease in adult acute myeloid leukemia is common but lacks independent significance: analysis of patients in ECOG-ACRIN cancer research group trials, 1980-2008. J Clin Oncol 2016;34:3544–53.
2. Röllig C, Ehninger G. How I treat hyperleukocytosis in acute myeloid leukemia. Blood 2015;125:3246–52.
3. Harris AC, Kitko CL, Couriel DR, Braun TM, Choi SW, Magenau J, et al. Extramedullary relapse of acute myeloid leukemia following allogeneic hematopoietic stem cell transplantation: incidence, risk factors and outcomes. Haematologica 2013;98:179–84.
4. Lai C, Doucette K, Norsworthy K. Recent drug approvals for acute myeloid leukemia. J Hematol Oncol 2019;12:100.
5. DiNardo CD, Pratz K, Pullarkat V, Jonas BA, Arellano M, Becker PS, et al. Venetoclax combined with decitabine or azacitidine in treatment-naive, elderly patients with acute myeloid leukemia. Blood 2019;133:7–17.
6. Bisaillon R, Moison C, Thiollier C, Krosl J, Bordeleau M-E, Lehnertz B, et al. Genetic characterization of ABT-199 sensitivity in human AML. Leukemia 2020;34:63–74.
7. Chau CH, Steeg PS, Figg WD. Antibody–drug conjugates for cancer. Lancet North Am Ed 2019;394:793–804.
8. Godwin CD, Gale RP, Walter RB. Gemtuzumab ozogamicin in acute myeloid leukemia. Leukemia 2017;31:1855–68.
9. Norsworthy KJ, Ko C-W, Lee JE, Liu J, John CS, Przepiorka D, et al. FDA approval summary: Mylotarg for treatment of patients with relapsed or refractory CD33-positive acute myeloid leukemia. Oncologist 2018;23:1103–8.
10. Pearce DJ, Taussig DC, Bonnet D. Implications of the expression of myeloid markers on normal and leukemic stem cells. Cell Cycle 2006;5:271–3.
11. Kovtun Y, Jones GE, Adams S, Harvey L, Audette CA, Wilhelm A, et al. A CD123-targeting antibody-drug conjugate, IMGN632, designed to eradicate AML while sparing normal bone marrow cells. Blood Adv 2018;2:848–58.
12. Jiang Y-P, Liu BY, Zheng Q, Panuganti S, Chen R, Zhu J, et al. CLT030, a leukemic stem cell-targeting CLL1 antibody-drug conjugate for treatment of acute myeloid leukemia. Blood Adv 2018;2:1738–49.
13. Hamblett KJ, Senter PD, Chace DF, Sun MMC, Lenox J, Cerveny CG, et al. Effects of drug loading on the antitumor activity of a monoclonal antibody drug conjugate. Clin Cancer Res 2004;10:7063–70.
14. Li F, Sutherland MK, Yu C, Walter RB, Westendorf L, Valliere-Douglass J, et al. Characterization of SGN-CD123A, a potent CD123-directed antibody-drug conjugate for acute myeloid leukemia. Mol Cancer Ther 2018;17:554–64.
15. Kang X, Kim J, Deng M, John S, Chen H, Wu G, et al. Inhibitory leukocyte immunoglobulin-like receptors: immune checkpoint proteins and tumor sustaining factors. Cell Cycle 2016;15:25–40.
16. Carosella ED, Rouas-Freiss N, Roux DT-L, Tronik-Le Roux D, Moreau P, LeMaoult J. HLA-G: an immune checkpoint molecule. Adv Immunol 2015;127:33–144.
17. Inui M, Hirota S, Hirano K, Fujii H, Sugahara-Tobinai A, Ishii T, et al. Human CD43+ B cells are closely related not only to memory B cells phenotypically but also to plasmablasts developmentally in healthy individuals. Int Immunol 2015;27:345–55.
18. John S, Chen H, Deng M, Gui X, Wu G, Chen W, et al. A novel anti-LILRB4 CAR-T cell for the treatment of monocytic AML. Mol Ther 2018;26:2487–95.
19. Deng M, Gui X, Kim J, Xie L, Chen W, Li Z, et al. LILRB4 signalling in leukaemia cells mediates T cell suppression and tumour infiltration. Nature 2018;562:605–9.
20. Dobrowolska H, Gill KZ, Serban G, Ivan E, Li Q, Qiao P, et al. Expression of immune inhibitory receptor ILT3 in acute myeloid leukemia with monocytic differentiation. Cytometry B Clin Cytom 2013;84:21–9.
21. Anami Y, Xiong W, Gui X, Deng M, Zhang CC, Zhang N, et al. Enzymatic conjugation using branched linkers for constructing homogeneous antibody-drug conjugates with high potency. Org Biomol Chem 2017;15:5635–42.
22. Anami Y, Tsuchikama K. Transglutaminase-mediated conjugations. Methods Mol Biol 2020;2078:71–82.
23. King HD, Yurgaitis D, Willner D, Firestone RA, Yang MB, Lasch SJ, et al. Monoclonal antibody conjugates of doxorubicin prepared with branched linkers: a novel method for increasing the potency of doxorubicin immunoconjugates. Bioconjugate Chem 1999;10:279–88.
24. Yasunaga M, Manabe S, Matsumura Y. New concept of cytotoxic immunoconjugate therapy targeting cancer-induced fibrin clots. Cancer Sci 2011;102:1396–402.
25. Anami Y, Yamazaki CM, Xiong W, Gui X, Zhang N, An Z, et al. Glutamic acid-valine-citrulline linkers ensure stability and efficacy of antibody-drug conjugates in mice. Nat Commun 2018;9:2512.
26. Gui X, Deng M, Song H, Chen Y, Xie J, Li Z, et al. Disrupting LILRB4/APOE interaction by an efficacious humanized antibody reverses T-cell suppression and blocks AML development. Cancer Immunol Res 2019;7:1244–57.
27. Reddy N, Ong GL, Behr TM, Sharkey RM, Goldenberg DM, Mattes MJ. Rapid blood clearance of mouse IgG2a and human IgG1 in many nude and nu/+ mouse strains is due to low IgG2a serum concentrations. Cancer Immunol Immunother 1998;46:25–33.
28. Cella M, Döhring C, Samaridis J, Dessing M, Brockhaus M, Lanzavecchia A, et al. A novel inhibitory receptor (ILT3) expressed on monocytes, macrophages, and dendritic cells involved in antigen processing. J Exp Med 1997;185:1743–51.
29. Lyon RP, Setter JR, Bovee TD, Doronina SO, Hunter JH, Anderson ME, et al. Self-hydrolyzing maleimides improve the stability and pharmacological properties of antibody-drug conjugates. Nat Biotechnol 2014;32:1059–62.
30. Taussig DC, Pearce DJ, Simpson C, Rohatiner AZ, Lister TA, Kelly G, et al. Hematopoietic stem cells express multiple myeloid markers: implications for the origin and targeted therapy of acute myeloid leukemia. Blood 2005;106:4086–92.
31. Seattle Genetics, Inc. Seattle Genetics discontinues phase 3 CASCADE trial of vadastuximab talirine (SGN-CD33A) in frontline acute myeloid leukemia. Available from: https://investor.seattlegenetics.com/press-releases/news-details/2017/Seattle-Genetics-Discontinues-Phase-3-CASCADE-Trial-of-Vadastuximab-Talirine-SGN-CD33A-in-Frontline-Acute-Myeloid-Leukemia/default.aspx.
32. Suciu-Foca N, Feirt N, Zhang Q-Y, Vlad G, Liu Z, Lin H, et al. Soluble Ig-like transcript 3 inhibits tumor allograft rejection in humanized SCID mice and T cell responses in cancer patients. J Immunol 2007;178:7432–41.
33. Barkal AA, Weiskopf K, Kao KS, Gordon SR, Rosental B, Yiu YY, et al. Engagement of MHC class I by the inhibitory receptor LILRB1 suppresses macrophages and is a target of cancer immunotherapy. Nat Immunol 2018;19:76–84.
34. Chen H-M, van der Touw W, Wang YS, Kang K, Mai S, Zhang J, et al. Blocking immunoinhibitory receptor LILRB2 reprograms tumor-associated myeloid cells and promotes antitumor immunity. J Clin Invest 2018;128:5647–62.
35. Kang X, Lu Z, Cui C, Deng M, Fan Y, Dong B, et al. The ITIM-containing receptor LAIR1 is essential for acute myeloid leukaemia development. Nat Cell Biol 2015;17:665–77.

36. Zhang CC, Fu Y-X. Another way to not get eaten. Nat Immunol 2018;19: 6–7.
37. Perna F, Berman SH, Soni RK, Mansilla-Soto J, Eyquem J, Hamieh M, et al. Integrating proteomics and transcriptomics for systematic combinatorial chimeric antigen receptor therapy of AML. Cancer Cell 2017;32:506–19.
38. Colovai AI, Tsao L, Wang S, Lin H, Wang C, Seki T, et al. Expression of inhibitory receptor ILT3 on neoplastic B cells is associated with lymphoid tissue involvement in chronic lymphocytic leukemia. Cytometry B Clin Cytom 2007;72:354–62.
39. Armstrong SA, Staunton JE, Silverman LB, Pieters R, Boer den ML, Minden MD, et al. MLL translocations specify a distinct gene expression profile that distinguishes a unique leukemia. Nat Genet 2002;30: 41–7.
40. de Goeje PL, Bezemer K, Heuvers ME, Dingemans A-MC, Groen HJ, Smit EF, et al. Immunoglobulin-like transcript 3 is expressed by myeloid-derived suppressor cells and correlates with survival in patients with non-small cell lung cancer. Oncoimmunology 2015;4:e1014242.
41. Chang CC, Ciubotariu R, Manavalan JS, Yuan J, Colovai AI, Piazza F, et al. Tolerization of dendritic cells by T(S) cells: the crucial role of inhibitory receptors ILT3 and ILT4. Nat Immunol 2002;3:237–43.
42. Brenk M, Scheler M, Koch S, Neumann J, Takikawa O, Häcker G, et al. Tryptophan deprivation induces inhibitory receptors ILT3 and ILT4 on dendritic cells favoring the induction of human CD4+CD25+ Foxp3+ T regulatory cells. J Immunol 2009;183:145–54.
43. Ge G, Tian P, Liu H, Zheng J, Fan X, Ding C, et al. Induction of CD4+ CD25+ Foxp3+ T regulatory cells by dendritic cells derived from ILT3 lentivirus-transduced human CD34+ cells. Transpl Immunol 2012;26:19–26.
44. Andersen MH. The targeting of immunosuppressive mechanisms in hematological malignancies. Leukemia 2014;28:1784–92.
45. Jeger S, Zimmermann K, Blanc A, Grünberg J, Honer M, Hunziker P, et al. Site-specific and stoichiometric modification of antibodies by bacterial transglutaminase. Angew Chem Int Ed 2010;49:9995–7.
46. Gorovits B, Krinos-Fiorotti C. Proposed mechanism of off-target toxicity for antibody-drug conjugates driven by mannose receptor uptake. Cancer Immunol Immunother 2013;62:217–23.
47. Doronina SO, Mendelsohn BA, Bovee TD, Cerveny CG, Alley SC, Meyer DL, et al. Enhanced activity of monomethylauristatin F through monoclonal antibody delivery: effects of linker technology on efficacy and toxicity. Bioconjugate Chem 2006;17:114–24.
48. Mirsalis JC, Schindler-Horvat J, Hill JR, Tomaszewski JE, Donohue SJ, Tyson CA. Toxicity of dolastatin 10 in mice, rats and dogs and its clinical relevance. Cancer Chemother Pharmacol 1999;44:395–402.
49. Lyon RP, Bovee TD, Doronina SO, Burke PJ, Hunter JH, Neff-LaFord HD, et al. Reducing hydrophobicity of homogeneous antibody-drug conjugates improves pharmacokinetics and therapeutic index. Nat Biotechnol 2015;33:733–5.
50. Viricel W, Fournet G, Beaumel S, Perrial E, Papot S, Dumontet C, et al. Monodisperse polysarcosine-based highly-loaded antibody-drug conjugates. Chem Sci 2019;10:4048–53.